Pea protein-coated nanoliposomal encapsulation of jujube phenolic extract with different stabilizers; characterization and *in vitro* release

Maedeh Parhizkary [a], Seid Mahdi Jafari [a,b,*], Elham Assadpour [c,d], Ayesheh Enayati [e], Mahboobeh Kashiri [a]

[a] *Faculty of Food Science and Technology, Gorgan University of Agricultural Sciences and Natural Resources, Gorgan, Iran*
[b] *Halal Research Center of IRI, Iran Food and Drug Administration, Ministry of Health and Medical Education, Tehran, Iran*
[c] *Food Industry Research Co., Gorgan, Iran*
[d] *Food and Bio-Nanotech International Research Center (Fabiano), Gorgan University of Agricultural Sciences and Natural Resources, Gorgan, Iran*
[e] *Golestan University of Medical Sciences, Gorgan, Iran*

A B S T R A C T

Jujube, a fruit rich in phenolic compounds, is renowned for its potential health benefits, including lowering blood pressure, and exhibiting anti-cancer, and anti-inflammatory effects, attributed to its potent antioxidant properties. However, the application of these phenolics in food products is limited by their instability and low concentration in plant tissues. This study investigates the nanoencapsulation of jujube extract (JE) using nanoliposomes (NLs) coated with pea protein isolate (PPI) to enhance stability and bioavailability. NLs were prepared *via* the ethanol injection method and optimized through comprehensive characterization, including dynamic light scattering, polydispersity index, and zeta potential. The encapsulated JE showed improved antioxidant activity and controlled release profiles in simulated gastric fluid and simulated intestinal fluid. This research highlights the potential of PPI-coated NLs in stabilizing and enhancing the bioactivity of jujube phenolics, providing a promising approach for their integration into functional foods.

1. Introduction

Jujube (*Ziziphus jujuba Mill.*), is considered the most important Ziziphus species for fruit production in the buckthorn family Rhamnaceae. It is native to China with a history of over 4000 years and is now widely distributed in Europe, southern and eastern Asia, and Australia. Renowned for its exceptional content of biologically active compounds, particularly phenolic compounds such as gallic acid, catechin and epicatechin, it offers significant nutritional and nutraceutical values (Gao et al., 2013). Phenolics are natural bioactive molecules mainly present in plant tissues. They form a significant portion of plant secondary metabolites, displaying distinct biological activities such as antioxidants, antimicrobials, and anti-inflammatory properties. The well-established antioxidant activity (AA) of phenolics has prompted extensive research and development for their utilization (Ribeiro et al., 2016).

Still, The food industry faces obstacles due to the low concentration of phenolics in plant tissues and the challenge of meeting the high demand from consumers (Cosme et al., 2020). Additionally, the vulnerability of phenolics to environmental factors such as light, heat, and oxygen may result in their degradation, causing a decline in their biological activities (Albuquerque & Heleno, 2021).

To address these limitations, encapsulation techniques are frequently employed to enhance the shelf life of phenolic compounds (Han et al., 2015). This procedure greatly improves phenolics' solubility, bioavailability, and resilience and prevents their degradation by external factors during processing and storage (Garavand et al., 2021). For this purpose, a variety of food carriers, such as polysaccharides, lipids, proteins, and surfactants, can be used to encapsulate phenolic compounds. However, it is crucial to ensure that encapsulated phenolics do not affect the color, flavor, or sensory attributes of the final product. More importantly, it is

necessary to select carriers that are natural, cost-effective, and generally recognized as safe (GRAS) for health (Tamjidi et al., 2013). Nanoliposomes (NLs) are a widely utilized form of nanocarriers, which are composed of two layers of phospholipids, trapping one or more hydrophilic and hydrophobic bioactive and they offer the capability to achieve controlled release of phenolics at precise locations and times (Bhattacharya et al., 2022). (Liu et al., 2020) demonstrated that NLs of β-carotene, vitamin C, and other bioactive all exhibited encapsulation efficiency (EE) > 60 %.

One of the techniques for preparing NLs is the ethanol injection approach, in which an organic (solvent) solution is injected into an aqueous (non-solvent) solution. This technique is preferred over other methods like Thin Film Hydration and Reverse Phase Evaporation, because the stability of prepared NLs by it is generally higher. Additionally, it is favored on an industrial scale due to its speed, safety, and

$$\text{Extraction Efficiency} = (\text{Weight of extract})/(\text{Initial sample weight}) \times 100 \tag{1}$$

Total phenolic content (TPC) was measured according to Zhou et al. (2023), and the results were expressed in terms of GA. In this method, Folin-Ciocalteu was used as the reagent. First, a calibration curve was drawn based on GA (within the range of 100 to 1000 ppm), and the absorbance of the samples was read at 760 nm. The DPPH radical scavenging assay was used to determine AA (Tan et al., 2014). Accordingly, 1.0 mL JE was mixed with 9.1 mL ethanol and 0.2 mL of a 0.5 mM DPPH solution. The resulting mixture was vortexed and left at room temperature for 30 min. Then, its absorption at 517 nm was measured. The scavenging rate of DPPH was calculated using Eq. 2. The control absorption was obtained by replacing the sample with ethanol. Distilled water was used as a blank sample.

$$\text{Scavenging of DPPH (\%)} = [1 - (\text{Absorbance of control/Absorbance of sample})] \times 100 \tag{2}$$

reproducibility (Shin et al., 2013). To enhance the stability and attain improved control over the release, a novel strategy is coating of NLs (Hasan et al., 2019). One of the biopolymers considered suitable for coating nanoliposomes (NLs) is pea protein, which exhibits numerous advantageous traits, particularly its plant-based origin and lack of allergens (Song et al., 2023). Pea protein isolate (PPI) possesses emulsification capability, which can be affected by its origin, extraction method, and environmental or processing factors like pH, ionic strength, and temperature (Burger & Zhang, 2019).

The purpose of this research was to nanoencapsulate jujube extract (JE) within optimized NLs and enhance their stability through PPI coating. Additionally, this paper provides an in-depth characterization of JE-loaded NLs, including analysis of particle size, polydispersity index (PDI), zeta potential (ZP), release kinetics, and morphology. These findings are expected to facilitate practical and efficient utilization of the developed NLs within the industry.

2. Materials and methods

2.1. Materials

The 96 % Ethanol was obtained from Kimia Alcohol (Zanjan, Iran), potassium acetate from Drmojallali Co., fish oil from Isfahan Research Center (Isfahan, Iran), ω3 from Dana Co., vitamin D from Gorgan Research Centre (Gorgan, Iran), and PPI from Saf Co. (Turkey). Other materials including sodium carbonate, aluminum chloride, Folin, DPPH, lecithin, β-sitosterol, cholesterol, monopotassium phosphate, Triton X-100, EDTA, sodium hydrogen carbonate, sodium chloride, pepsin, hydrochloric acid, pancreatin, sodium hydroxide and Tween 80 (Tw) were purchased from Merck (Germany).

2.2. Extraction of jujube extract and its properties

For obtaining JE, the method utilized was adapted from Tian et al. (2017) with minor adjustments. Essentially, the de-seeded fruit powder underwent filtration through a mesh size of 60. Subsequently, 50 g jujube powder was mixed with 500 mL ethanol/water solvent (80:20). It was then agitated on a shaker at 180 rpm for 24 h at room temperature. Next, JE underwent filtration using Whatman filter paper No.1 and concentrated *via* a rotary evaporator (IKA, Germany). Ultimately, the concentrated JE was dried using a freeze-dryer (Operon, South Korea). The extraction efficiency was determined by Eq. 1 (Han et al., 2015).

Finally, the phenolic profile of JE was characterized by high performance liquid chromatography (HPLC).

2.3. Loading jujube phenolic extract into nanoliposomes

NLs were prepared using the ethanol injection method, as described by Toniazzo et al. (2017), with slight modifications. The organic phase, consisting of a specific ratio of lecithin to Tw (10 and 20 mg) and 10 mg stabilizers (ω3, cholesterol, fish oil, and β-sitosterol) heated in ethanol at 60 °C, and mixed by a magnetic stirrer. Then, JE (40/20 mg) was dissolved in 20 mL of preheated deionized water (aqueous phase). The organic phase was then injected into the aqueous phase by a syringe. The resulting sample was sonicated (70 % power and 0.5 cycles) for 30 min (6 s on and 3 s off). After the characterization of NLs (Section 2.5), the sample with ω3 stabilizer and 0.01 Tw was selected as the optimal one for coating. For the preparation of PPI-coated NLs (C-NLs), different concentrations of PPI (0.1, 0.2, 0.4 % *w/v*) dissolved in 20 mL of preheated deionized water and added drop-wise into NLs solutions under a magnetic stirring at 500 rpm for 1 h, followed by static standing of the mixture for 0.5 h to ensure the complete combination of PPI with NLs (Tai et al., 2020). Afterward, the dispersion solution was sonicated. Different samples with relevant codes are shown in Table 1.

2.4. Characterization of loaded nanoliposomes

The mean particle size, PDI, and ZP of NLs were measured using a dynamic light scattering (DLS) instrument (Nanosizer 3000, Malvern

Table 1
Various treatments and sample codes in this study.

Nanocarrier	Stabilizer	Tween concentration (%)	Sample code
Nanoliposomes (NLs)	Cholesterol	0.1	CH-$T_{0.1}$
		0.2	CH-$T_{0.2}$
	Fish oil	0.1	FI- $T_{0.1}$
		0.2	FI- $T_{0.2}$
	Omega 3 fatty acids	0.1	ω-$T_{0.1}$
		0.2	ω-$T_{0.2}$
	β-sitosterol	0.1	β-$T_{0.1}$
		0.2	β-$T_{0.2}$
	Coating biopolymer	**Coating concentration (%)**	
Coated nanoliposomes (C-NLs)	Pea protein isolate	0.1	$C_{0.1}$-NLs
		0.2	$C_{0.2}$-NLs
		0.4	$C_{0.4}$-NLs

Instruments, UK). To avoid multiple scattering, each sample (1 mL) was diluted with distilled water in a 100-fold ratio. The measurement was conducted at 25 °C with an angle of 90 ^{0} and a wavelength of 633 nm (Sarabandi, Mahoonak, et al., 2019). For the separation of the non-encapsulated phenolics from NLs suspension, centrifugation at 3000 rpm for 15 min was employed. The absorption levels in both fractions were measured using a spectrophotometer at 760 nm, and EE was calculated using Eq. 3(Flamminii et al., 2021).

$$Encapsulation\,Efficiency\,(\%) = [1 - Unencapsulated\,drug/Total\,drug] \times 100 \tag{3}$$

Subsequently, AA was calculated using the DPPH scavenging method (Tan et al., 2014).

The optimized samples, comprising loaded and empty NLs, C-NLs along with JE, ω3, Tw, and PPI underwent FTIR analysis within the range of 4000 to 400 cm^{-1} using an FTIR spectrophotometer (Shimadzu 8400, Japan)(Zhang et al., 2022). For evaluating the structure and morphology of all NLs, scanning electron microscopy was employed. In this process, a 100-μL NLs suspension was dried on a glass slide. The selected sample was subsequently coated with gold, and imaging was conducted (Sarabandi, Jafari, et al., 2019).

2.5. Release of phenolics from nanoliposomes

In summary, dialysis bags were immersed in a simulated gastric fluid (SGF) containing 2.0 % sodium chloride and 32.0 % pepsin by weight. The pH was adjusted to 2 using a 5.0 M hydrochloric acid solution. The SGF was maintained in a shaking incubator at 37 °C for 2 h, with periodic sampling every 30 min(Hasan et al., 2018). After 2 h digestion in SGF, dialysis bags were transferred to a simulated intestinal fluid (SIF), which contained 0.1 % pancreatin and 50 mM potassium dihydrogen phosphate. The pH of SIF was adjusted to 8.6 with 5.0 M sodium hydroxide. Then, they were placed in a shaking incubator at 37 °C for 4 h, with sampling every 30 min (Hasan et al., 2019).

2.6. Statistical analysis

The findings from this study were subjected to statistical analysis using a completely randomized design with three replications, employing SPSS software version 26. The means were compared using the Duncan test at a significance level of 0.05 ($P \leq 0.05$). Furthermore, graphical illustrations were generated using Microsoft Office Excel 2019.

Table 2
Summary of HPLC data.

| Peak IDs	Retention Time (min)	Peak area (%)	Recovery (%)	Concentration (mg/100 g)
Gallic Acid	3.44	22.644	98	153.357
Catechin	4.31	8.366	94	27.836
Epicatechin	5.26	9.939	99	31.044
Rutin	7.21	7.733	96	18.714
Quercitrin	9.67	3.618	90	4.337
m-Coumaric Acid	10.18	6.524	98	12.711
Quercetin	13.71	9.258	94	28.215
Caffeic Acid	14.23	13.342	93	61.370
Chlorogenic Acid	15.19	18.572	98	112.023

3. Results and discussion

3.1. The extraction efficiency of jujube extract and its properties

The extraction efficiency of JE was 84.76 % based on dry matter, which was slightly lower than those reported by Farahani (2019) According to HPLC analysis, as shown in Fig. 1 and Table 2, GA was identified as the primary phenolic compound in the JE. TPC in the powder of ethanol JE was 28.531 mg GA equivalent (GAE)/g dry weight, which is comparable to the range reported by Zhou et al. (2023), approximately from 18.11 to 21 mg/g. The DPPH scavenging rate of JE was 86.16 %. (Li et al., 2005) found DPPH scavenging for various jujube varieties from 33.6 % to 98.6 %.

3.2. Properties of loaded nanoliposomes

The nanoliposomes utilized in this research were multivesicular vesicles (MVVs), which enable the encapsulation of multiple substances within distinct vesicles in them. This structural complexity not only enhances the versatility of the delivery system but also significantly improves the stability of the encapsulated materials. The crucial factors
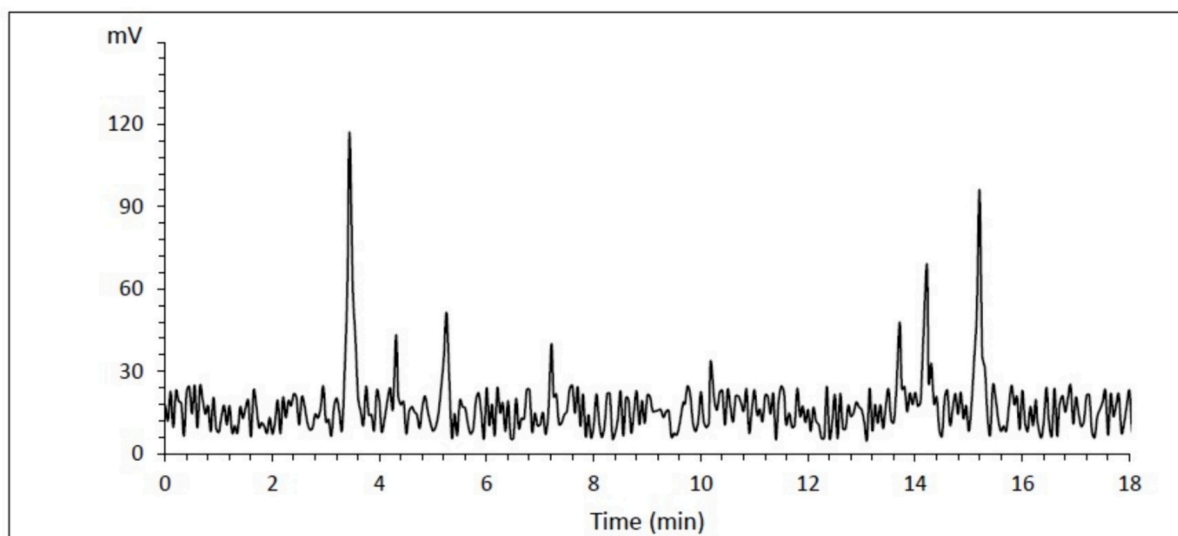
Fig. 1. The HPLC chromatogram of the jujube extract.

determining the characteristics of NLs are their size and PDI. Factors influencing the size of NLs include concentrations of phospholipids, stabilizers, and the use of various non-ionic surfactants (Shaker et al., 2017). In this study, the smallest and largest sizes of NLs corresponded to treatments ω-$T_{0.2}$ and β-$T_{0.1}$ with sizes of 109 ± 0.87 nm and 345 ± 0.26 nm, respectively. Increasing the amount of Tw leads to a smaller size of NLs due to its amphiphilic nature. Higher concentrations of Tw increase

the curvature of the NLs' outer bilayer membrane, resulting in a more spherical shape. The hydrophilic head of Tw interacts with the aqueous environment, while its hydrophobic tail inserts into the lipid bilayer. This insertion disrupts the packing of the lipids in the bilayer, increasing the curvature. Tw molecules create a more disordered and flexible membrane structure, enhancing the overall curvature of the nano-liposome bilayer, ultimately resulting in smaller NL sizes. However, with
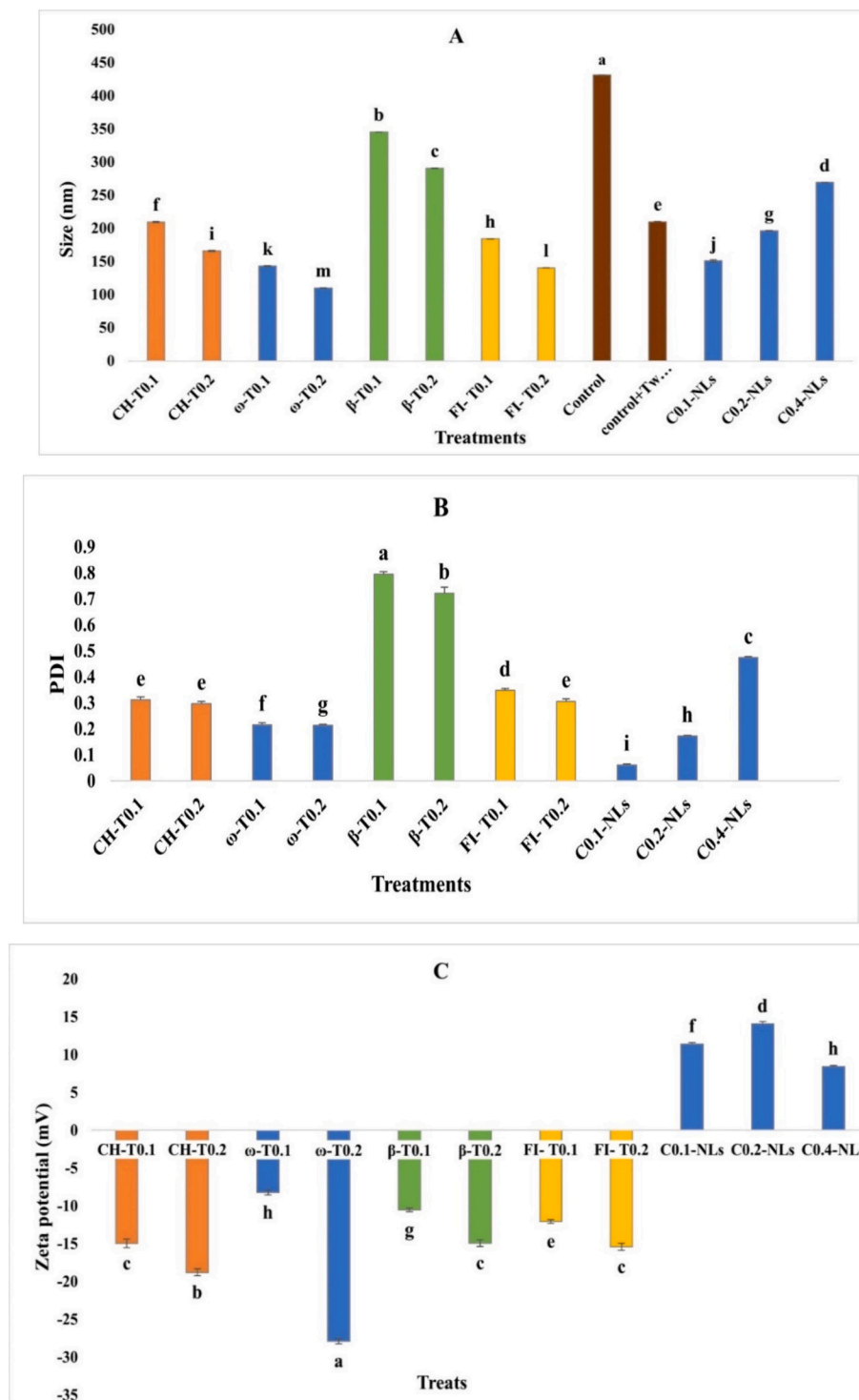
Fig. 2. (A) Particle size, (B) polydispersity index (PDI), and (C) zeta potential of different nanoliposomes (NLs); identical letters indicate no statistically significant difference between treatments at $P > 0.05$ (CH-$T_{0.1}$ and CH-$T_{0.2}$: NLs with cholesterol stabilizer and 0.1 % or 0.2 % Tw; ω-$T_{0.1}$ and ω-$T_{0.2}$: ω3 and 0.1 % or 0.2 % Tw; β-$T_{0.1}$ and β-$T_{0.2}$: β-sitosterol and 0.1 % or 0.2 % Tw; FI- $T_{0.1}$ and FI- $T_{0.2}$: fish oil and 0.1 % or 0.2 % Tw; Control: NLs without Tw and stabilizer, Control + Tw: NLs without stabilizer and with Tw); $C_{0.1}$-NLs, $C_{0.2}$-NLs, $C_{0.4}$-NLs refers to NLs coated with 0.1, 0.2, and 0.4 % pea protein).

a decrease in Tw, NLs lose their spherical shape and become more irregular, leading to an increase in their size. This trend was also supported by Fan et al. (2008).

In this study, two natural sterols as stabilizers of NLs were β-sitosterol and cholesterol. They contribute to maintaining the integrity and stability of NLs by incorporating them into the lipid bilayer. Among treatments, the highest particle size was observed for β-$T_{0.1}$ and β-$T_{0.2}$ treatments, which were stabilized by β-sitosterol. Following these treatments, CH-$T_{0.1}$ was stabilized by cholesterol. The larger size of NLs containing sterols compared to other samples is attributed to the interaction of sterols with the lipid chains close to the phospholipid head groups, forming space between lipids and expanding the membrane (Jovanović et al., 2018). For example, sterols, due to their cyclic structure, have larger particle sizes than ω3 and fish oil. Among sterols, β-sitosterol, and cholesterol have similar chemical structures, both being hydrophobic in the core and hydrophilic at the head. However, cholesterol is smaller (with a molecular weight (Mw) = 386.65 g/mol) and stiffer, while β-sitosterol has a larger structure (Mw = 414.71 g/mol) and is more flexible. Compared to other stabilizers (fish oil and ω3), ω3 resulted in a smaller particle size. The combination between ω3 and Tw is particularly effective in reducing surface tension and preventing particle aggregation. It also promotes the formation of smaller and more stable particles compared to other treatments. Fish oil is a complex mixture of ω3 fatty acids, phospholipids, and other components. The presence of these additional lipids in fish oil may lead to the formation of larger NLs compared to those stabilized only with ω3 fatty acids.

In the next step, by coating NLs with different PPI concentrations (0.1, 0.2, and 0.4 %), the size of all samples increased, similar to studies by Song et al. (2023), where a higher coating material concentration led to an increase in particle size. As shown in Fig. 2A, the size of NLs after coating ranged from 104 ± 1.70 nm for sample $C_{0.1}$-NLs to 268 ± 0.40 nm for sample $C_{0.4}$-NLs, all of which differed significantly ($P < 0.05$) with the uncoated NLs (142 ± 0.87 nm). The higher size of C-NLs is attributed to the increase in the thickness of the protein layer on the lipid membrane (Ramezanzade et al., 2017).

In the work by Hanafy et al. (2015), the effect of 80 % Tw in retention of particle size and PDI during short-term (one week) and long-term (3 months) storage of NLs was confirmed. Therefore, in all treatments of this study, Tw was used at two different ratios. we found that an increase in Tw resulted in a reduction of these indices. As depicted in Fig. 2B, the PDI of treatments CH-$T_{0.1}$ and CH-$T_{0.2}$ were 0.311 ± 0.013 and 0.296 ± 0.008, respectively. Still, they did not differ significantly ($P > 0.05$), which was consistent with the data of Nowroozi et al. (2018) regarding the PDI of cholesterol treatments. Although cholesterol may harm the human body, it has been analyzed in this research for comparative purposes (Guo et al., 2024). The effects of sterols on PDI vary due to their different chemical compositions. For example, in β-$T_{0.1}$ and β-$T_{0.2}$ samples, PDI was significantly higher than those containing cholesterol due to the difference in sterol structures. Notably, the lowest PDI was associated with treatment ω-$T_{0.2}$, which showed no significant difference with ω-$T_{0.1}$. On the other hand, the highest PDI was linked to treatment β-$T_{0.1}$.

Furthermore, all C-NLs differed significantly ($P < 0.05$) from each other and the uncoated NLs. The lowest PDI was observed in treatment $C_{0.1}$-NLs, while the highest PDI was related to treatment $C_{0.4}$-NLs. Based on these values, coating of NLs with 0.1 % and 0.2 % PPI led to a lower PDI, while coating with 0.4 % PPI caused an increase in PDI, which was also observed by Pan et al. (2020), indicating the relatively homogeneous distribution of NLs after coating and attributing it to protein adsorption and NLs aggregation. However, since a PDI ≤ 3.0 is acceptable and indicates greater uniformity in the samples, treatment with 0.4 coatings was considered unacceptable.

By comparing the particle size distributions and their ZP, it can be observed that NLs with a common stabilizer, which had smaller particle sizes, had a higher absolute ZP because with an increase in particle size, the surface-to-volume ratio increases, leading to a higher charge density

on the particle surfaces(Nakatuka et al., 2015). Consequently, the electrostatic repulsion between NLs increases, resulting in reduced aggregation and increased stability (Das & Das, 2022). In this study, we had different ZP values due to the diversity of stabilizers. For example, treatments of ω-$T_{0.1}$ and ω-$T_{0.2}$ had a negative ZP because they contain fatty acids whose carboxylic acid group ionizes at pH > 5.4. The significant reduction in ZP can be explained by the fact that carboxylic acid groups of fatty acids are positioned more on the surface due to conformational changes during encapsulation, leading to a better formation of NLs. Consequently, treatment ω-$T_{0.2}$ showed a significant decrease in ZP (-27.8 ± 0.36 mV). Similarly, treatments β-T0.1 and β-T0.2 exhibited negative ZPs. This negative ZP arises from the interaction of β-sitosterol with phospholipid head groups through hydrogen bonding, which reduces electrostatic repulsion between the head groups. However, incorporating them enhances hydrophobic interactions with acyl chains, which can further stabilize the bilayers.

NLs formulated with cholesterol (CH-$T_{0.1}$ and CH-$T_{0.2}$) also showed negative ZP (-14.80 ± 0.56 and -3.19 ± 0.45 mV, respectively), which were similar to the study of Németh et al. (2022) in the range of -17.10 to -6.32 mV. It has occurred due to the formation of hydrogen bonds between the hydroxyl group of cholesterol and the choline of lecithin, creating dipole-dipole attractions. Treatments with fish oil (FI-$T_{0.1}$ and FI-$T_{0.2}$) had ZP of -13.12 ± 0.25 and -6.15 ± 0.47 mV, respectively. Additionally, biopolymers with opposite charges are used for coating of NLs. In this study, PPI had a ZP = $+17.56 \pm 0.39$ mV similar to the data of Helmick et al. (2021), where the ZP of PPI ranged from -30 to $+30$ mV. As shown in Fig. 2C, treatment $C_{0.4}$-NLs did not significantly differ ($P > 0.05$) from the absolute value of the uncoated optimal NLs, indicating low interaction at this concentration. However, all of the C-NLs exhibited significant differences from each other and the uncoated NLs, indicating a transition from a negative to a positive ZP. These changes in ZP after protein coating indicate electrostatic interactions, which are the main driving force for the successful coating of NLs(De Villiers et al., 2011).

Treatments CH-$T_{0.1}$ and CH-$T_{0.2}$, which contained cholesterol, had relatively low EE (35.66 % and 40.45 %, respectively), as shown in Fig. 3A. Another influential factor on EE in this study was the level of Tw; a higher Tw level decreased the EE, which could be attributed to the complete destruction of NL layers due to encapsulated material leakage. However, in the study of Fan et al. (2008), due to the hydrophobicity of the encapsulated compound, a slight increase in Tw led to higher EE because it increased the surface density of NLs and availability of the lipid-friendly environment. The lowest EE was observed in treatments with β-sitosterol (β-$T_{0.1}$ and β-$T_{0.2}$), which were 32.13 % and 29.15 %, respectively. As shown in Fig. 3A, the highest EE was related to treatments ω-$T_{0.1}$, ω-$T_{0.2}$, and FI-$T_{0.1}$, which were 73.76 %, 64.75 %, and 71.71 %, respectively, consistent with the findings of Caddeo et al. (2008).

The size of carriers significantly impacts the success of the encapsulation process. While sizes between 50 and 150 nm are generally recommended, larger sizes have also been observed. The size of carriers and EE are closely related due to the surface area-to-volume ratio and diffusion path length. Smaller carriers, with their larger surface area, interact more effectively with the encapsulating bioactive, leading to higher EE (Aguilar-Pérez et al., 2020). However, extremely small carriers may also lead to encapsulated material leakage or instability. Conversely, larger carriers may have lower EE due to a reduced surface area for interaction and a longer diffusion path for the core material, but they may provide better stability. For example, NLs made with ω3, which had the smallest size, had the highest EE. This aligns with the findings of Jøraholmen et al. (2015), who discovered NLs with larger sizes had lower EE. Regarding C-NLs, there was a significant difference ($P < 0.05$) in EE between them and the uncoated NLs. Moreover, there was an increase in EE after coating, which gradually decreased at a higher PPI level. Higher EE after coating up to a certain concentration in the study by Pan et al. (2020) was attributed to the effective prevention
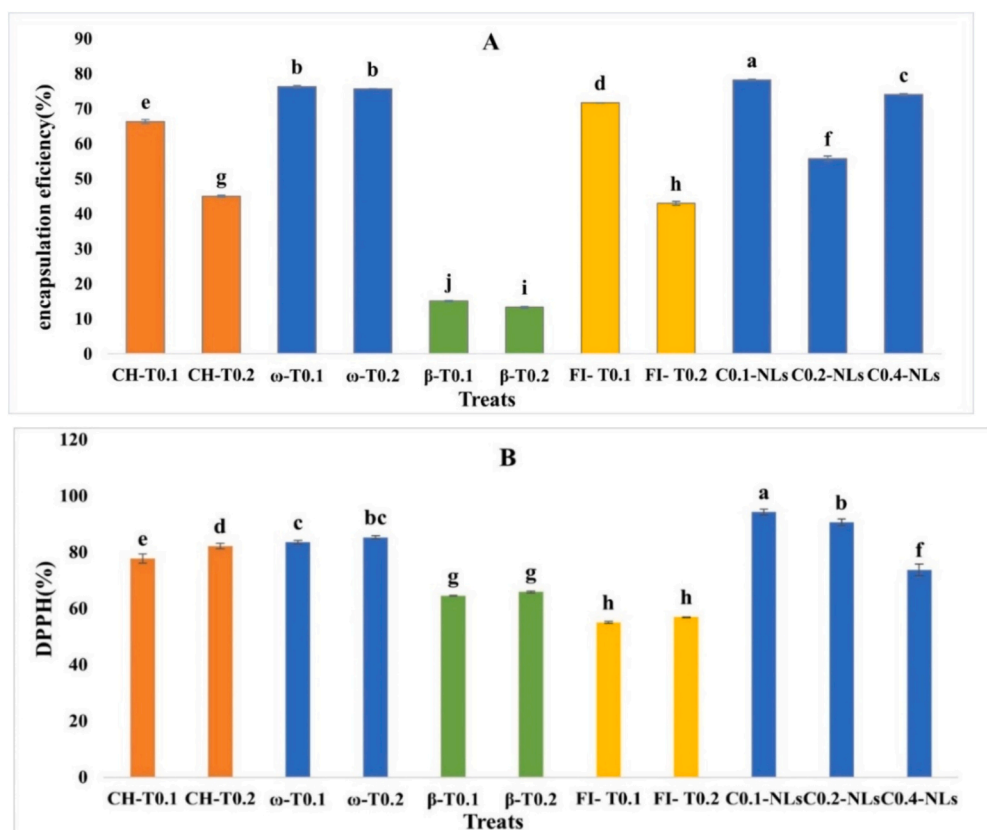
Fig. 3. (A) Encapsulation efficiency and **(B)** DPPH scavenging rate of different nanoliposomes (NLs); identical letters indicate no statistically significant difference between treatments at $P > 0.05$ (CH-$T_{0.1}$ and CH-$T_{0.2}$: NLs with cholesterol stabilizer and 0.1 % or 0.2 % Tw; ω-$T_{0.1}$ and ω-$T_{0.2}$: ω3 and 0.1 % or 0.2 % Tw; β-$T_{0.1}$ and β-$T_{0.2}$: β-sitosterol and 0.1 % or 0.2 % Tw; FI- $T_{0.1}$ and FI- $T_{0.2}$: fish oil and 0.1 % or 0.2 % Tw); $C_{0.1}$-NLs, $C_{0.2}$-NLs, $C_{0.4}$-NLs refers to NLs coated with 0.1, 0.2, and 0.4 % pea protein).

of encapsulated material leakage from the NLs lipid membrane by the coated layer during the preparation process.

As shown in Fig. 3B, the DPPH scavenging activity before encapsulation was 16.86 ± 0.74 %, which significantly increased within the NLs, particularly in the ω-T0.1 and ω-T0.2 treatments, where it reached 85 ± 0.62 %. This substantial enhancement in DPPH scavenging post-encapsulation suggests that the encapsulation process significantly improves the AA of the compounds. This could be attributed to the protective environment provided by NLs, which helps to maintain the stability and integrity of the encapsulated antioxidants, thereby preventing oxidation. On the other hand, a decrease in DPPH scavenging was observed for other treatments (FI-T0.1, CH-T0.1, CH-T0.2, FI-T0.2, β-T0.1, and β-T0.2) following EE. Tan et al. (2013) also reported higher antioxidant activity after encapsulation, suggesting that non-coated NLs are more prone to oxidation due to unsaturated fatty acids in their phospholipids.

### 3.3. The release of jujube phenolics from nanoliposomes

The release of phenolics from different NLs under SGF and SIF conditions is shown in Fig. 4, revealing that the surfactant and stabilizer had a significant effect on the release ($P < 0.05$). Under SGF, the highest release (3.41 ± 0.25 mg/g) after 2.0 h was related to treatment β-T0.2, followed by treatments Ch-T0.2 and β-T0.1 (2.67 ± 0.34 and 3.24 ± 0.25 mg/g, respectively). According to Fig. 4i, the lowest release was related to FI-T0.1 treatment. At a higher surfactant level (Tw), the release increased while its stability decreased. Surfactants can reduce the surface tension between NLs and their surrounding environment, facilitating effective dispersion and release of loaded bioactive. Therefore, NLs with higher Tw content exhibited greater release, as reported by Fan

et al. (2008).

On the other hand, stabilizers help NLs maintain their structural integrity and prevent aggregation or premature leakage of their contents. They form a protective layer on the surface of NLs, which reduces direct contact between liposomes and minimizes the risk of aggregation. By imparting electrostatic charges onto the surface of NLs, stabilizers create repulsive forces that help maintain separation between liposomes, thus preventing aggregation. Additionally, stabilizers create a physical barrier around NLs, increasing the distance between individual liposomes and further reducing the likelihood of aggregation. Furthermore, stabilizers interact with the lipid bilayer of NLs, enhancing their rigidity and reducing the likelihood of membrane disruption, which helps to prevent leakage of encapsulated contents. (Tasi et al., 2003) stated that the use of Tw increases the stability of NLs. Therefore, Tw was used in all treatments in this study. Used stabilizers had a significant difference ($P < 0.05$) in terms of release rate. Furthermore, as shown in Fig. 4i(B), the highest release (5.33 ± 0.38 mg/g) under SIF, similar to the stomach, was attributed to treatment ω-T0.1; whereas the lowest release (2.44 ± 0.46 mg/g) was related to treatment β-T0.2 which was contrary to SGF, indicating the low impact of β-sitosterol due to low release in the intestine.

According to Kushnazarova et al. (2021), two influential factors affecting the release are the extent of interactions between loaded bioactive and the NLs membrane and their permeability (increased fluidity of the membrane leads to the release of loaded bioactive into the surrounding environment). One of the stabilizers used in this study was cholesterol, which has been proven to be effective in the stability of NLs. Therefore, they also have a significant impact on controlling the release. In general, all treatments had a higher release in the intestine, which is probably due to the presence of pancreatin in SIF capable of hydrolyzing
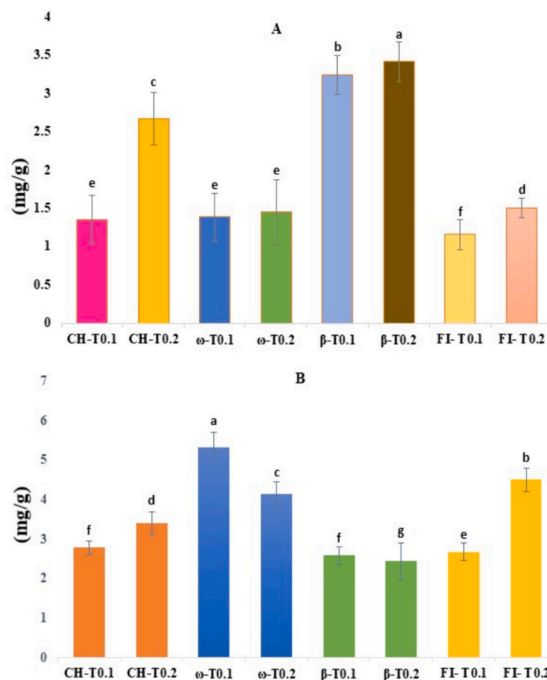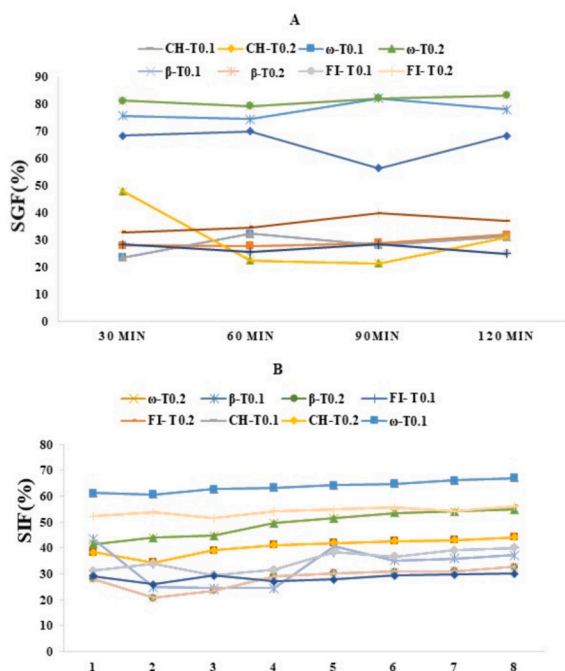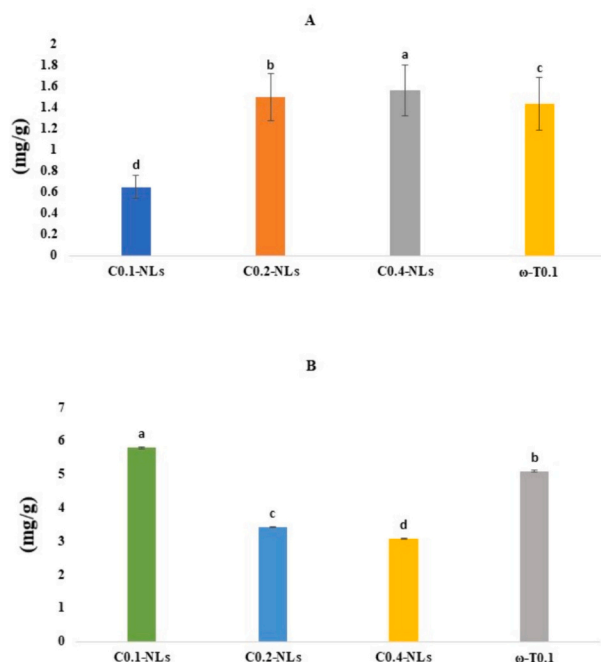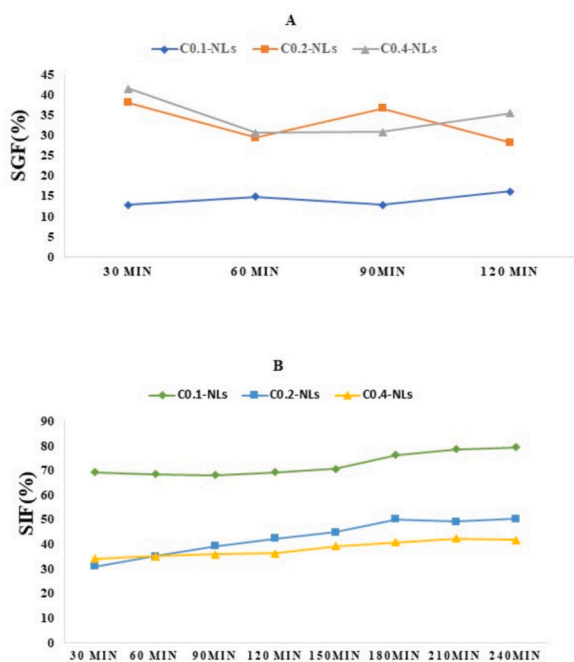
Fig. 4. (i) Release of loaded nanoliposomes (NLs) with jujube extract in SGF (A) and SIF (B) conditions (CH-$T_{0.1}$ and CH-$T_{0.2}$: NLs with cholesterol stabilizer and 0.1 % or 0.2 % Tw; ω-$T_{0.1}$ and ω-$T_{0.2}$: ω3 and 0.1 % or 0.2 % Tw; β-$T_{0.1}$ and β-$T_{0.2}$: β-sitosterol and 0.1 % or 0.2 % Tw; FI- $T_{0.1}$ and FI- $T_{0.2}$: fish oil and 0.1 % or 0.2 % Tw); **(ii)** Release of phenolic compounds from coated nanoliposomes in SGF (A) and SIF (B) environments ($C_{0.1}$-NLs, $C_{0.2}$-NLs, $C_{0.4}$-NLs refers to NLs coated with 0.1, 0.2, and 0.4 % pea protein); similar letters indicate no statistically significant difference between treatments at $P > 0.05$.

lipid compounds present in the NLs membrane. Additionally, in the intestine, due to the forces generated by intestinal movement, they are emulsified, leading to faster action of pancreatic enzymes in the breakdown of NLs, resulting in membrane degradation and faster release of loaded bioactive (Salehi et al., 2022).

After coating, the highest release under SGF was related to treatment $C_{0.4}$-NLs, while the lowest release was related to treatment $C_{0.1}$-NLs, which also had a lower release than uncoated NLs (Fig. 4ii). In the study by Hasan et al. (2019), the rate of drug release in SGF decreased for chitosan-coated NLs, which is a desirable feature for protecting

bioactive molecules against the harsh gastric environment. Under SIF, the highest release was attributed to treatment $C_{0.1}$-NLs, indicating the successful delivery of JE to the target site; while other treatments in this environment even had less release than the optimal non-coated NLs.

3.4. Morphological characteristics of nanoliposomes

In the study of Amnuaikit et al. (2018), who used ethanol injection method, the morphological shapes of NLs were similar to those in our study (Fig. 5i). In SEM images corresponding to β-$T_{0.1}$ and β-$T_{0.2}$
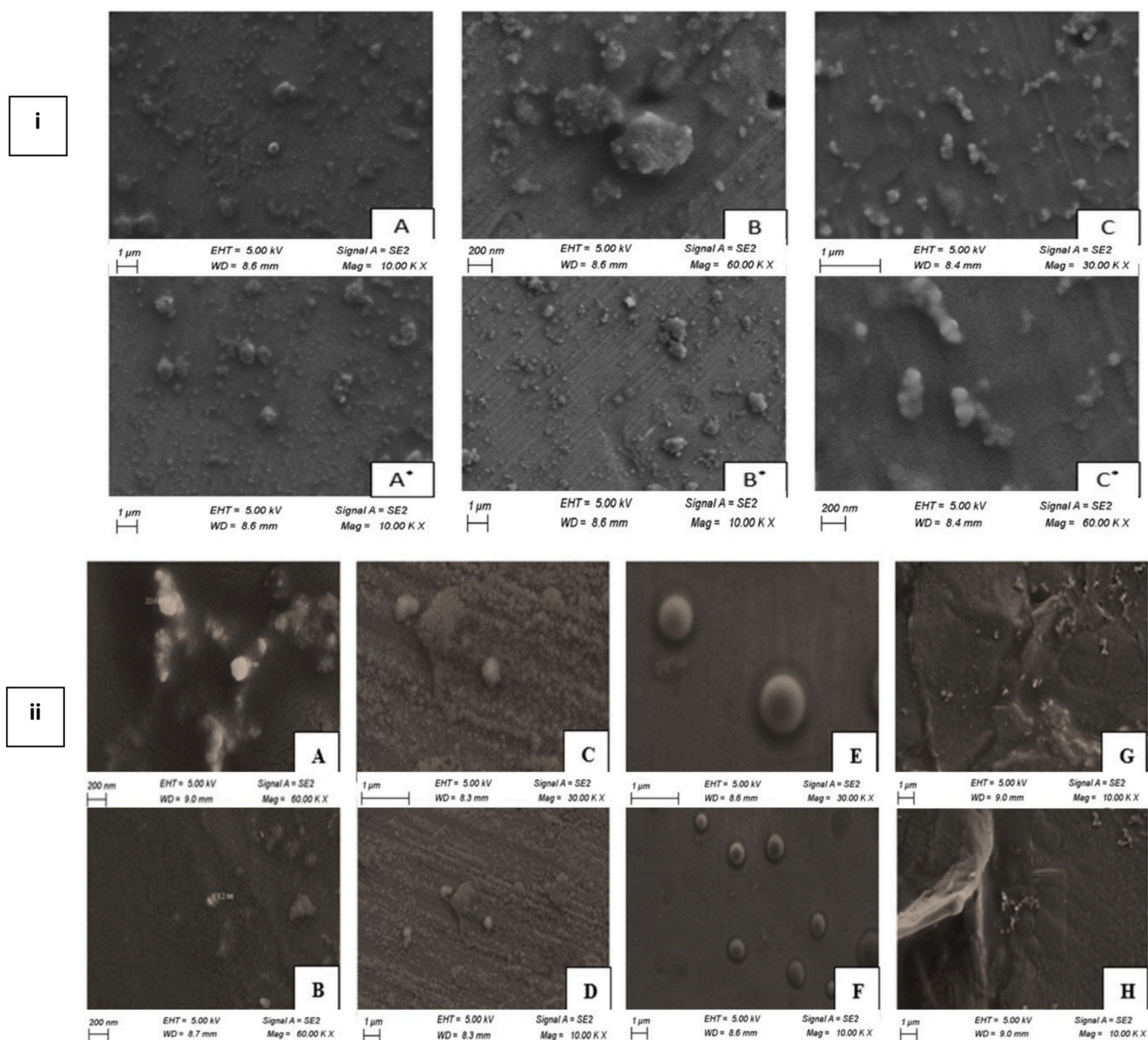
Fig. 5. (i) SEM images of coated nanoliposomes (A and A*: treatment $C_{0.1}$-NLs, B and B*: treatment $C_{0.2}$-NLs, and C and C*: treatment $C_{0.4}$-NLs); **(ii)** SEM images of non-coated nanoliposomes (A and B: treatments β-$T_{0.1}$ and β-$T_{0.2}$, C and D: treatments FI- $T_{0.1}$ and FI- $T_{0.2}$, E and F: treatments CH-$T_{0.1}$ and CH-$T_{0.2}$ and G and H: treatments ω-$T_{0.1}$ and ω-$T_{0.2}$).

treatments (Fig. 5i(A and B)), it can be observed that a small number of NLs had a spherical shape without smooth surfaces. In the SEM images related to FI-$T_{0.1}$ and FI-$T_{0.2}$ treatments (Fig. 5i(C and D)), a greater number of NLs are formed, and they exhibit smoother surfaces. For CH-$T_{0.1}$ and CH-$T_{0.2}$ treatments (Fig. 5i(E and F)), the number of NLs is lower, but they are larger and have smooth surfaces. The images related to the optimal samples ω-$T_{0.1}$ and ω-$T_{0.2}$ (Fig. 5i(G and H)) show a higher number of NLs, mostly in spherical shape, with smaller sizes and better dispersion. As evident in Fig. 5i, the vesicular shape is more prevalent in NLs with cholesterol and ω3 stabilizers.

Fig. 5ii depicts the SEM images of C-NLs. The $C_{0.1}$-NLs showed a higher vesicular state compared to other NLs, and in $C_{0.4}$-NLs, we observed aggregation of NLs, which was predictable based on the PDI associated with this treatment. Generally, after coating with PPI, the number of NLs formed increased, and their spherical nature was enhanced, particularly in $C_{0.1}$-NLs. Moreover, this sample exhibited a

smoother surface compared to other C-NLs.

3.5. Chemical interactions

The results of FTIR spectroscopy for the optimal NLs (treatment ω-$T_{0.1}$), both loaded and unloaded, as well as JE, ω3, and Tw are shown in Fig. 6A. In the spectrum corresponding to JE, the characteristic peaks were observed at 1049, 1626, and 3433 cm^{-1}. The first peak, at 1049 cm^{-1}, signifies alkyl halides (groups with C—H bonds) and amines, indicating stretching vibrations of C—N (aliphatic amines) and carboxylic acids. Esters are also identified in this peak, displaying C—O stretching vibrations as two or more bands in the range of 1300–1000 cm^{-1}. The subsequent peak in the JE spectrum, at 1626 cm^{-1}, indicates amides, possessing characteristics of amines (Shao & Tang, 2016) and ketones. This peak also suggests the presence of alkenes (C=C bond stretching vibrations) and amine groups (N—H bending, primary amines
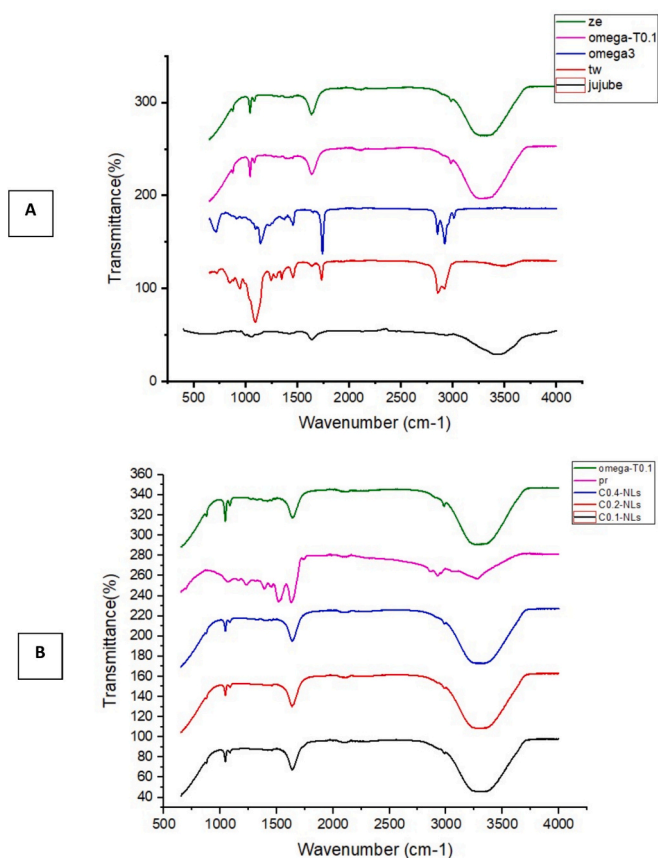
Fig. 6. FTIR spectra of **(A)** loaded nanoliposomes (NLs) with jujube extract, unloaded NLs, and jujube extract.

only). The last peak (3433 cm^{-1}) confirms the presence of alcohols and phenols, with hydrogen bonding (O—H stretching) in the range of 3500–3200 cm^{-1}. Similar peaks were found by Golmohammadi et al. (2020), with a strong and broad characteristic peak at 1342 cm^{-1}, indicating O—H stretching vibrations. Additionally, peaks at 2925 and 1425 cm^{-1}, corresponding to CH$_2$ and C—C, respectively, were identified and attributed to aromatic ring structures.

The FTIR spectra of empty and loaded NLs exhibited remarkable similarities (Fig. 6A). Soleimanifar et al. (2020) also noted minor differences between loaded and unloaded NLs, indicating successful encapsulation of the bioactive. The observed peaks in these NLs were at 1042, 1642, and 2395 cm^{-1}. The first peak suggests the presence of alkyl halides that exhibit C—F stretching vibrations in the range of 1350–1000 cm^{-1}. This peak also indicates the presence of amino compounds (aliphatic amine C—N stretching vibrations). The subsequent peak at 1642 cm^{-1} signifies alkenes, displaying C═C stretching vibrations, and amides similar to those found in the JE spectrum. The final peak (2395 cm^{-1}) indicates alkynes, carboxylic acids, and amines, as well as alcohols and phenols, consistent with the previous findings. Comparing the FTIR spectra of empty (zero) and optimal (ω-T$_{0.1}$) NLs, an increase in peak intensity was observed which is indicative of the presence of JE in NLs. Furthermore, the location of the peaks, resembling those in the JE spectrum, further confirms the incorporation of JE into NLs.

(Ze: NLs without extract, omega-T$_{0.1}$: NLs with 0.1 % Tw and ω3 stabilizer, jujube: non-liposomal jujube extract, omega3: the ω3 stabilizer alone, and Tw: Tw alone); **(B)** non-coated nanoliposomes loaded with jujube extract (ω3 and 0.1 % Tw) and coated nanoliposomes containing jujube extract C$_{0.1}$-NLs, C$_{0.2}$-NLs, C$_{0.4}$-NLs refers to NLs coated with 0.1, 0.2, and 0.4 % pea protein, and pure pea protein (Pr)

In the spectrum of PPI (Fig. 6B), the peak at 1607 cm^{-1} indicates the

presence of amides. A similar peak was observed by Saxton and McDougal (Saxton & McDougal, 2021) for PPI. In this region, in the spectrum corresponding to the optimal non-coated NLs (ω3), the peak at 1625 cm^{-1} signifies the presence of amides, amines, and alkenes, which after coating, was confirmed by the peak at 1636 cm^{-1} indicating the presence of amides and amines. In the spectrum of PPI, the peak at 1062 cm^{-1} corresponds to alkyl halides and amines, which in the optimal non-coated NLs (ω3) was reflected by the peak at 1043 cm^{-1}, indicating the same compounds. After coating, an additional peak appeared between these two peaks at 1053 cm^{-1}, confirming the presence of alkyl halides, amines, and additionally alcohols. The production of alcohol from alkyl halides and amines can be attributed to a process known as nucleophilic substitution, involving the reaction of an alkyl halide with an amine to form an alkylamine intermediate, which can further undergo reactions to produce alcohol. The next peak in the PPI spectrum (at 3282 cm^{-1}) corresponds to alkenes and carboxylic acids, which in non-coated NLs (ω3) is represented by the peak at 3295 cm^{-1}, indicating similar compounds. Overall, in the spectrum of the optimal C-NLs (C$_{0.1}$-NLs), the intensity of the peaks decreased, indicating successful coating by PPI.

4. Conclusion

This research successfully demonstrated the nanoencapsulation of JE into NLs and further stabilized them with PPI. Phenolics, particularly those derived from jujube, are notable for their antioxidant, antimicrobial, and anti-inflammatory properties but are highly sensitive to environmental conditions. The encapsulation process using NLs provided a protective barrier against factors such as oxygen, light, and free radicals, significantly enhancing the stability and bioavailability of these phenolic compounds. Among the various stabilizers tested, ω3 exhibited the best performance with the highest EE of 76.238 ± 0.23 % and minimal release in SGF. The optimal formulation, ω3-T-0.1, demonstrated an EE of 78.19 ± 0.21 % and the lowest release in SGF, making it suitable for further industrial applications. Moreover, this study provided an in-depth characterization of JE-loaded NLs, analyzing particle size, PDI, ZP, release kinetics, and morphology. The findings revealed that coating the NLs with different concentrations of PPI improved their stability, with 0.1 % PPI being the most effective. The successful encapsulation and enhanced stability of JE in NLs provide a promising method for integrating bioactive compounds into food products, ensuring their effectiveness, and prolonging their shelf life. While the materials used in this study are considered safe, further research is needed to evaluate long-term toxicity, chronic effects, and potential mechanisms of action. These insights pave the way for the practical and efficient utilization of NLs in the food industry, potentially leading to healthier and more stable functional foods.

CRediT authorship contribution statement

Maedeh Parhizkary: Methodology, Investigation, Formal analysis, Data curation. **Seid Mahdi Jafari:** Writing – review & editing, Visualization, Validation, Supervision, Project administration. **Elham Assadpour:** Writing – review & editing, Validation, Formal analysis. **Ayesheh Enayati:** Writing – review & editing, Validation, Methodology. **Mahboobeh Kashiri:** Writing – review & editing, Validation, Methodology.

Declaration of competing interest

The authors declare that there is no conflict of interest related with this work.

Data availability

The data that has been used is confidential.

References

Aguilar-Pérez, K. M., Avilés-Castrillo, J. I., Medina, D. I., Parra-Saldivar, R., & Iqbal, H. M. N. (2020). Insight into Nanoliposomes as smart Nanocarriers for greening the twenty-first century biomedical settings. *Frontiers in Bioengineering and Biotechnology, 8*, Article 579536. https://doi.org/10.3389/FBIOE.2020.579536/BIBTEX

Albuquerque, B. R., Heleno, S. A., Oliveira, M. B. P. P., Barros, L., & Ferreira, I. C. F. R. (2021). Phenolic compounds: Current industrial applications, limitations and future challenges. *Food & Function, 12*(1), 14–29. https://doi.org/10.1039/D0FO02324H

Amnuaikit, T., Limsuwan, T., Khongkow, P., & Boonme, P. (2018). Vesicular carriers containing phenylethyl resorcinol for topical delivery system; liposomes, transfersomes and invasomes. *Asian Journal of Pharmaceutical Sciences, 13*(5), 472–484. https://doi.org/10.1016/J.AJPS.2018.02.004

Bhattacharya, S., Saindane, D., & Prajapati, B. G. (2022). Liposomal drug delivery and its potential impact on Cancer research. *Anti-Cancer Agents in Medicinal Chemistry, 22*(15), 2671–2683. https://doi.org/10.2174/1871520622666220418141640

Burger, T. G., & Zhang, Y. (2019). Recent progress in the utilization of pea protein as an emulsifier for food applications. *Trends in Food Science and Technology, 86*, 25–33. https://doi.org/10.1016/J.TIFS.2019.02.007

Caddeo, C., Teskač, K., Sinico, C., & Kristl, J. (2008). Effect of resveratrol incorporated in liposomes on proliferation and UV-B protection of cells. *International Journal of Pharmaceutics, 363*(1–2), 183–191. https://doi.org/10.1016/J.IJPHARM.2008.07.024

Cosme, P., Rodríguez, A. B., Espino, J., & Garrido, M. (2020). Plant Phenolics: Bioavailability as a key determinant of their potential health-promoting applications. *Antioxidants (Basel, Switzerland), 9*(12), 1–20. https://doi.org/10.3390/ANTIOX9121263

Das, P., & Das, M. K. (2022). Production and physicochemical characterization of nanocosmeceuticals. *Nanocosmeceuticals: Innovation, Application, and Safety*, 95–138. https://doi.org/10.1016/B978-0-323-91077-4.00006-5

De Villiers, M. M., Otto, D. P., Strydom, S. J., & Lvov, Y. M. (2011). Introduction to nanocoatings produced by layer-by-layer (LbL) self-assembly. *Advanced Drug Delivery Reviews, 63*(9), 701–715. https://doi.org/10.1016/J.ADDR.2011.05.011

Fan, M., Xu, S., Xia, S., & Zhang, X. (2008). Preparation of salidroside nano-liposomes by ethanol injection method and in vitro release study. *European Food Research and Technology, 227*(1), 167–174. https://doi.org/10.1007/S00217-007-0706-9

Farahani, Z. K. (2019). *Halal edible biopolymers used in food encapsulation: A review*. https://doi.org/10.30502/jhhhm.2021.283062.1032

Flamminii, F., Paciulli, M., Di Michele, A., Littardi, P., Carini, E., Chiavaro, E., … Di Mattia, C. D. (2021). Alginate-based microparticles structured with different biopolymers and enriched with a phenolic-rich olive leaves extract: A physicochemical characterization. *Current Research in Food Science, 4*, 698–706. https://doi.org/10.1016/J.CRFS.2021.10.001

Gao, Q. H., Wu, C. S., & Wang, M. (2013). The jujube (Ziziphus jujuba mill.) fruit: A review of current knowledge of fruit composition and health benefits. *Journal of Agricultural and Food Chemistry, 61*(14), 3351–3363. https://doi.org/10.1021/JF4007032

Garavand, F., Jalai-Jivan, M., Assadpour, E., & Jafari, S. M. (2021). Encapsulation of phenolic compounds within nano/microemulsion systems: A review. *Food Chemistry, 364*. https://doi.org/10.1016/J.FOODCHEM.2021.130376

Golmohammadi, M., Honarmand, M., & Ghanbari, S. (2020). A green approach to synthesis of ZnO nanoparticles using jujube fruit extract and their application in photocatalytic degradation of organic dyes. *Spectrochimica Acta Part A: Molecular and Biomolecular Spectroscopy, 229*, Article 117961. https://doi.org/10.1016/J.SAA.2019.117961

Guo, J., Chen, S., Zhang, Y., Liu, J., Jiang, L., Hu, L., Yao, K., Yu, Y., & Chen, X. (2024). Cholesterol metabolism: Physiological regulation and diseases. *MedComm, 5*(2), Article e476. https://doi.org/10.1002/MCO2.476

Han, H. J., Lee, J. S., Park, S. A., Ahn, J. B., & Lee, H. G. (2015). Extraction optimization and nanoencapsulation of jujube pulp and seed for enhancing antioxidant activity. *Colloids and surfaces. B, Biointerfaces, 130*, 93–100. https://doi.org/10.1016/J.COLSURFB.2015.03.050

Hanafy, A. S., Farid, R. M., & Elgamal, S. S. (2015). Complexation as an approach to entrap cationic drugs into cationic nanoparticles administered intranasally for Alzheimer's disease management: Preparation and detection in rat brain. *Drug Development and Industrial Pharmacy, 41*(12), 2055–2068. https://doi.org/10.3109/03639045.2015.1062897

Hasan, M., Elkhoury, K., Kahn, C. J. F., Arab-Tehrany, E., & Linder, M. (2019). Preparation, characterization, and release kinetics of chitosan-coated nanoliposomes encapsulating curcumin in simulated environments. *Molecules, 24*(10). https://doi.org/10.3390/MOLECULES24102023

Hasan, M., Latifi, S., Kahn, C. J. F., Tamayol, A., Habibey, R., Passeri, E., … Arab-Tehrany, E. (2018). The positive role of curcumin-loaded Salmon Nanoliposomes on the culture of primary cortical neurons. *Marine Drugs, 16*(7). https://doi.org/10.3390/MD16070218

Helmick, H., Hartanto, C., Bhunia, A., Liceaga, A., & Kokini, J. L. (2021). Validation of Bioinformatic modeling for the zeta potential of Vicilin, Legumin, and commercial pea protein isolate. *Food Biophysics, 16*(4), 474–483. https://doi.org/10.1007/S11483-021-09686-8

Jøraholmen, M. W., Škalko-Basnet, N., Acharya, G., & Basnet, P. (2015). Resveratrol-loaded liposomes for topical treatment of the vaginal inflammation and infections. *European Journal of Pharmaceutical Sciences : Official Journal of the European Federation for Pharmaceutical Sciences, 79*, 112–121. https://doi.org/10.1016/J.EJPS.2015.09.007

Jovanović, A. A., Balanč, B. D., Ota, A., Ahlin Grabnar, P., Djordjević, V. B., Šavikin, K. P., … Poklar Ulrih, N. (2018). Comparative effects of cholesterol and β-Sitosterol on the liposome membrane characteristics. *European Journal of Lipid Science and Technology, 120*(9). https://doi.org/10.1002/EJLT.201800039

Kushnazarova, R. A., Mirgorodskaya, A. B., & Zakharova, L. Y. (2021). Niosomes modified with cationic surfactants to increase the bioavailability and stability of indomethacin. *Russian Chemical Bulletin, 70*(3), 585–591. https://doi.org/10.1007/S11172-021-3129-Z/METRICS

Li, J. W., Ding, S. D., & Ding, X. L. (2005). Comparison of antioxidant capacities of extracts from five cultivars of Chinese jujube. *Process Biochemistry, 40*(11), 3607–3613. https://doi.org/10.1016/J.PROCBIO.2005.03.005

Liu, X. X., Liu, H. M., Yan, Y. Y., Fan, L. Y., Yang, J. N., de Wang, X., & Qin, G. Y. (2020). Structural characterization and antioxidant activity of polysaccharides extracted from jujube using subcritical water. *LWT, 117*. https://doi.org/10.1016/J.LWT.2019.108645

Nakatuka, Y., Yoshida, H., Fukui, K., & Matuzawa, M. (2015). The effect of particle size distribution on effective zeta-potential by use of the sedimentation method. *Advanced Powder Technology, 26*(2), 650–656. https://doi.org/10.1016/J.APT.2015.01.017

Németh, Z., Csóka, I., Semnani Jazani, R., Sipos, B., Haspel, H., Kozma, G., … Dobó, D. G. (2022). Quality by design-driven zeta potential optimisation study of liposomes with charge imparting membrane additives. *Pharmaceutics, 14*(9). https://doi.org/10.3390/PHARMACEUTICS14091798

Nowroozi, F., Almasi, A., Javidi, J., Haeri, A., & Dadashzadeh, S. (2018). Effect of surfactant type, cholesterol content and various downsizing methods on the particle size of Niosomes. *Iranian Journal of Pharmaceutical Research : IJPR, 17*(Suppl2), 1. /pmc/articles/PMC6447874/.

Pan, L., Zhang, X., Fan, X., Li, H., Xu, B., & Li, X. (2020). Whey protein isolate coated liposomes as novel carrier Systems for Astaxanthin. *European Journal of Lipid Science and Technology, 122*(4), 1900325. https://doi.org/10.1002/EJLT.201900325

Ramezanzade, L., Hosseini, S. F., & Nikkhah, M. (2017). Biopolymer-coated nanoliposomes as carriers of rainbow trout skin-derived antioxidant peptides. *Food Chemistry, 234*, 220–229. https://doi.org/10.1016/J.FOODCHEM.2017.04.177

Ribeiro, A., Caleja, C., Barros, L., Santos-Buelga, C., Barreiro, M. F., & Ferreira, I. C. F. R. (2016). Rosemary extracts in functional foods: Extraction, chemical characterization and incorporation of free and microencapsulated forms in cottage cheese. *Food & Function, 7*(5), 2185–2196. https://doi.org/10.1039/C6FO00270F

Salehi, S., Nourbakhsh, M. S., Yousefpour, M., Rajabzadeh, G., & Sahab-Negah, S. (2022). Co-encapsulation of curcumin and boswellic acids in chitosan-coated niosome: An in-vitro digestion study. *Journal of Microencapsulation, 39*(3), 226–238. https://doi.org/10.1080/02652048.2022.2060360

Sarabandi, K., Jafari, S. M., Mahoonak, A. S., & Mohammadi, A. (2019). Application of gum Arabic and maltodextrin for encapsulation of eggplant peel extract as a natural antioxidant and color source. *International Journal of Biological Macromolecules, 140*, 59–68. https://doi.org/10.1016/J.IJBIOMAC.2019.08.133

Sarabandi, K., Mahoonak, A. S., Hamishehkar, H., Ghorbani, M., & Jafari, S. M. (2019). Protection of casein hydrolysates within nanoliposomes: Antioxidant and stability characterization. *Journal of Food Engineering, 251*, 19–28. https://doi.org/10.1016/J.JFOODENG.2019.02.004

Saxton, R., & McDougal, O. M. (2021). Whey protein powder analysis by mid-infrared spectroscopy. *Foods, 10*(5). https://doi.org/10.3390/FOODS10051033/S1

Shaker, S., Gardouh, A., & Ghorab, M. (2017). Factors affecting liposomes particle size prepared by ethanol injection method. *Research in Pharmaceutical Sciences, 12*(5), 346. https://doi.org/10.4103/1735-5362.213979

Shao, Y., & Tang, C. H. (2016). Gel-like pea protein Pickering emulsions at pH 3.0 as a potential intestine-targeted and sustained-release delivery system for β-carotene. *Food Research International, 79*, 64–72. https://doi.org/10.1016/J.FOODRES.2015.11.025

Shin, G. H., Chung, S. K., Kim, J. T., Joung, H. J., & Park, H. J. (2013). Preparation of chitosan-coated nanoliposomes for improving the mucoadhesive property of curcumin using the ethanol injection method. *Journal of Agricultural and Food Chemistry, 61*(46), 11119–11126. https://doi.org/10.1021/JF4035404

Soleimanifar, M., Jafari, S. M., & Assadpour, E. (2020). Encapsulation of olive leaf phenolics within electrosprayed whey protein nanoparticles; production and characterization. *Food Hydrocolloids, 101*. https://doi.org/10.1016/J.FOODHYD.2019.105572

Song, F., Chen, J., Zhang, Z., & Tian, S. (2023). Preparation, characterization, and evaluation of flaxseed oil liposomes coated with chitosan and pea protein isolate hydrolysates. *Food Chemistry, 404*, Article 134547. https://doi.org/10.1016/J.FOODCHEM.2022.134547

Tai, K., Rappolt, M., Mao, L., Gao, Y., Li, X., & Yuan, F. (2020). The stabilization and release performances of curcumin-loaded liposomes coated by high and low molecular weight chitosan. *Food Hydrocolloids, 99*, Article 105355. https://doi.org/10.1016/J.FOODHYD.2019.105355

Tamjidi, F., Shahedi, M., Varshosaz, J., & Nasirpour, A. (2013). Nanostructured lipid carriers (NLC): A potential delivery system for bioactive food molecules. *Innovative*

Food Science & Emerging Technologies, 19, 29–43. https://doi.org/10.1016/J.IFSET.2013.03.002

Tan, C., Xue, J., Abbas, S., Feng, B., Zhang, X., & Xia, S. (2014). Liposome as a delivery system for carotenoids: Comparative antioxidant activity of carotenoids as measured by ferric reducing antioxidant power, DPPH assay and lipid peroxidation. *Journal of Agricultural and Food Chemistry, 62*(28), 6726–6735. https://doi.org/10.1021/JF405622F/ASSET/IMAGES/MEDIUM/JF-2013-05622F_0006.GIF

Tasi, L. M., Liu, D. Z., & Chen, W. Y. (2003). Microcalorimetric investigation of the interaction of polysorbate surfactants with unilamellar phosphatidylcholines liposomes. *Colloids and Surfaces A: Physicochemical and Engineering Aspects, 213*(1), 7–14. https://doi.org/10.1016/S0927-7757(02)00287-X

Tian, Y., Liimatainen, J., Alanne, A. L., Lindstedt, A., Liu, P., Sinkkonen, J., … Yang, B. (2017). Phenolic compounds extracted by acidic aqueous ethanol from berries and leaves of different berry plants. *Food Chemistry, 220*, 266–281. https://doi.org/10.1016/J.FOODCHEM.2016.09.145

Toniazzo, T., Peres, M. S., Ramos, A. P., & Pinho, S. C. (2017). Encapsulation of quercetin in liposomes by ethanol injection and physicochemical characterization of dispersions and lyophilized vesicles. *Food Bioscience, 19*, 17–25. https://doi.org/10.1016/J.FBIO.2017.05.003

Zhang, Y., Cai, P., Cheng, G., & Zhang, Y. (2022). A brief review of phenolic compounds identified from plants: Their extraction, analysis, and biological activity. *Natural Product Communications, 17*(1). doi: 10.1177/1934578X211069721/ASSET/IMAGES/LARGE/10.1177_1934578X211069721-FIG 1.JPEG.

Zhou, X., Zhang, Z., Pu, Y., Wu, C., Yan, M., & Zhang, Q. (2023). Study on the spatial specificity of phenolics in fruit of different jujube varieties. *Scientific Reports 2023 13: 1, 13*(1), 1–11. https://doi.org/10.1038/s41598-023-46228-3